PCP
PLANT & CELL PHYSIOLOGY

Rapid Paper

Proteasome Inhibition in *Brassica napus* Roots Increases Amino Acid Synthesis to Offset Reduced Proteolysis

Dan Pereksta[1], Dillon King[1,4], Fahmida Saki[1,5], Amith Maroli[2], Elizabeth Leonard[2], Vidya Suseela[2], Sean May[3], Marcos Castellanos Uribe[3], Nishanth Tharayil[2] and Doug Van Hoewyk[1,*]

[1]Biology Department, Coastal Carolina University, 107 Chanticleer Drive, Conway, SC 29526, USA
[2]Department of Agriculture and Environmental Sciences, Clemson University, 105 Collins Street, Clemson, SC 29634, USA
[3]School of Biosciences, University of Nottingham, Loughborough LE12 5RD, UK
[4]Present address: Toxicology and Environmental Health. Duke University. 225 B Wing, Levine Science Research Center Durham, North Carolina 27708, USA
[5]Present address: National Technical Institute for the Deaf 52 Lomb Memorial Dr, Rochester, NY 14623, USA

Microarray data are deposited at the GEO (Gene Expression Omnibus) archive and can be accessed (GSE127923).

*Corresponding author: E-mail, dougvh@coastal.edu; Fax, +1-843-349-2201.

(Received December 10, 2019; Accepted April 10, 2020)

Cellular homeostasis is maintained by the proteasomal degradation of regulatory and misfolded proteins, which sustains the amino acid pool. Although proteasomes alleviate stress by removing damaged proteins, mounting evidence indicates that severe stress caused by salt, metal(oids), and some pathogens can impair the proteasome. However, the consequences of proteasome inhibition in plants are not well understood and even less is known about how its malfunctioning alters metabolic activities. Lethality causes by proteasome inhibition in non-photosynthetic organisms stem from amino acid depletion, and we hypothesized that plants respond to proteasome inhibition by increasing amino acid biosynthesis. To address these questions, the short-term effects of proteasome inhibition were monitored for 3, 8 and 48 h in the roots of *Brassica napus* treated with the proteasome inhibitor MG132. Proteasome inhibition did not affect the pool of free amino acids after 48 h, which was attributed to elevated de novo amino acid synthesis; these observations coincided with increased levels of sulfite reductase and nitrate reductase activities at earlier time points. However, elevated amino acid synthesis failed to fully restore protein synthesis. In addition, transcriptome analysis points to perturbed abscisic acid signaling and decreased sugar metabolism after 8 h of proteasome inhibition. Proteasome inhibition increased the levels of alternative oxidase but decreased aconitase activity, most sugars and tricarboxylic acid metabolites in root tissue after 48 h. These metabolic responses occurred before we observed an accumulation of reactive oxygen species. We discuss how the metabolic response to proteasome inhibition and abiotic stress partially overlap in plants.

Keywords: Alternative oxidase • Amino acids • Nitrogen metabolism • Oxidative stress • Protein synthesis • Sulfite reductase • TCA cycle • Ubiquitin.

Introduction

Protein turnover allows for plasticity in sessile plants during a variety of developmental and environmental changes. Abiotic stress can result in the accumulation of oxidized and misfolded proteins that need to be either repaired or removed from cells. While autophagy is responsible for the bulk degradation of proteins, the targeted removal of selected proteins in eukaryotes is achieved by the proteasomes, which have been best characterized in yeast and human cells (Finley 2009). The 26S proteasome is composed of a 20S proteolytic core bound by either one or two ATP-dependent 19S regulatory particles (Yang et al. 2004). To ensure specificity during proteolysis, proteins delivered to the 26S proteasome are tagged with the highly conserved protein ubiquitin, which is dependent upon the concerted action of ubiquitin E1-activating enzymes, E2-conjugating enzymes and E3 ligases that transfer ubiquitin onto the target protein.

Proteolysis of ubiquitinated proteins by proteasomes serves a variety of functions (Vierstra 2003). In addition to clearing damaged proteins from eukaryotic cells, proteasomes degrade many short-lived regulatory proteins, perhaps most famously those governing cell division in animals and plants (Genschik et al. 1998, Ekholm and Reed 2000). It is also estimated that ~30% of newly synthesized proteins in eukaryotic cells are malformed and undergo rapid proteasomal degradation; this serves to prevent cytotoxic protein aggregation and maintain the levels of free amino acids (Schubert et al. 2000). In plants, the proteasome regulates a myriad of abiotic stress responses (Lyzenga and Stone 2012). During abiotic stress, oxidized and misfolded proteins are cleared by the 20S and 26S proteasomes, respectively, thereby preventing accumulation of toxic protein aggregates. For example, proteasome can clear nonspecific and misfolded selenoproteins containing a cysteine-to-selenocysteine substitution (Sabbagh and Van Hoewyk 2012). Proteasomes also govern plant development, including microtubule-mediated formation (Sheng et al. 2006, Wang et al. 2011), seed germination (Chiu et al. 2016) and processes dependent upon hormone signaling (Santner and Estelle 2009), such as jasmonate-mediated root elongation (Valenzuela et al. 2016). Arabidopsis mutants with defects in

Plant Cell Physiol. 61(6): 1028–1040 (2020) doi:10.1093/pcp/pcaa047, Advance Access publication on 20 April 2020, available online at https://academic.oup.com/pcp

the 26S proteasome are viable but exhibit delayed development (Kurepa et al. 2008) likely due to the perturbation of the multitude of cellular and developmental processes regulated by proteasomes.

The cellular and physiological effects of proteasome inhibition in plants are not well-characterized, in contrast to yeast and mammalian cells (Chung et al. 2001). Proteasome inhibition leads to protein aggregation causing an unfolded protein response (Bush et al. 1997). Furthermore, proteasome inhibition decreases protein synthesis in a wide variety of organisms (Ding et al. 2006, Suraweera et al. 2012). Severe and prolonged proteasome inhibition is cytotoxic and generates reactive oxygen species (ROS), including superoxide (Maharjan et al. 2015) that can ultimately lead to apoptosis in Arabidopsis (Kim et al. 2003). Proteasome inhibition in the green algae *Chlamydomonas* exacerbates sensitivity to high light, nickel and selenium (Vallentine et al. 2014, Mendoza et al. 2020); these studies further implicate the importance of proteasomes in mediating abiotic stress tolerance in plants.

Recently, it was proposed that lethality stemming from prolonged proteasome inhibition in heterotrophic cells is not directly a consequence of ROS accumulation (Ling et al. 2003) or protein aggregation (Bence et al. 2001) but is rather a result of amino acid starvation (Suraweera et al. 2012), which is abated by amino acid supplementation. Proteasome inhibition in Arabidopsis results in autophagy and degradation of inactive proteasomes (Sheng et al. 2012, Marshall et al. 2015), which might counteract decreased proteolysis and prevent the depletion of free amino acids. It was also observed by Svozil et al. (2015) that levels of nitrate reductase (NR) accumulate in proteasome-inhibited plants, possibly to support amino acid synthesis. However, this hypothesis has not been experimentally tested.

We sought to address the disparity in our understanding of how heterotrophs and autotrophic plants respond to proteasome inhibition. We broadly sought to answer how plants reconfigure cellular activities to offset the consequences of proteasome inhibition. We specifically questioned if plants are able to prevent amino acid depletion by increasing nitrogen metabolism to support de novo amino acid synthesis, which would help alleviate the toxic effects of proteasome impairment. We discuss how these questions are particularly salient to our understanding of plant stress physiology, as salt (Wang et al. 2011, Han et al. 2019), metal(oids) (Pena et al. 2008, Karmous et al., 2014, Dimkovikj and Van Hoewyk 2014) and pathogens (Groll et al., 2008) can impair proteasome activity.

Results

Proteasome inhibition stunts plant growth and development

Initial experiments focused on establishing the toxic effects of the proteasome inhibitor MG132 in young seedlings. Seven-day-old seedlings were treated with 50 μM MG132, a concentration that has previously been used to inhibit the proteasome in *B. napus* and Arabidopsis (Dimkovikj and Van Hoewyk 2014, Marshall et al. 2015). MG132 treatment for 2 d increased root length but decreased hypocotyl length (**Fig. 1A** and **Table 1**). However, this shift in growth between the roots and hypocotyl did not affect the fresh weight or length of seedlings compared to untreated plants at day 2. After 10 d, the effects of proteasome inhibition were more pronounced. MG132 stunted the growth of seedlings, as demonstrated by the 20% decrease in plant length and the 55% decrease in fresh weight. Although the chlorophyll content was not affected, plants treated with MG132 had decreased Fv/Fm, which represents the maximum capacity of photosystem II in dark-adapted plants. In addition, starch levels nearly doubled in the leaves of MG132-treated plants after 10 d (**Table 1**) and can be visualized by the iodine–starch complex that stained the leaf tissue blue (**Fig. 1B**). Taken together, these data indicate that a nonlethal concentration of 50 μM MG132 induced stress and altered the physiology and development of *B. napus* plants.

Subsequent experiments focused on determining the short-term consequences of proteasome inhibition in *B. napus* roots, because this is the organ system first exposed to salt and metals that can impair proteasome activity. Therefore, experiments were performed in 4-week-old plants to ensure more biomass for analyses and were designed to examine the early effects of proteasome inhibition in roots treated with 50 μM MG132 for 3, 8 and 48 h. MG132 treatment decreased proteasome activity by 94–96% (**Fig. 2A**), which resulted in the accumulation of high-molecular-weight ubiquitinated proteins (**Fig. 2B**) and an increase in total protein at all time points (**Fig. 2C**).

Proteasome inhibition alters metabolite profiles and decreases protein synthesis

We used a metabolomics approach to understand how proteasome inhibition (the suppression of a major proteolytic pathway) affects levels of amino acid and central carbon metabolites in *B. napus* roots. Surprisingly, after 48 h, there was almost a 2-fold increase in asparagine and glutamine, the first amino acid synthesized in the nitrogen assimilation pathway, as well as a subtle (nonsignificant) increase in most measured amino acids (**Fig. 3A** and **Supplementary Table S1**). However, we observed a decrease in aspartate and glutamate, which, respectively, are substrates for asparagine and glutamine synthetase and precursors for other amino acids. After 48 h of proteasome inhibition, the peak ratios of asparagine:aspartate and glutamine:glutamate more than doubled (**Fig. 3B**). MG132 also strongly induced an accumulation of shikimate—a metabolic precursor for aromatic amino acids—at all time points. There was a decrease in dehydroascorbic acid (DHA) and most soluble sugars, including galactose from which DHA is synthesized. Also, noteworthy is a reduction in the levels of most TCA cycle intermediates at 3 and 48 h. The decrease in TCA cycle metabolites at these early time points coincided with a decrease in the activity of aconitase, an enzyme that participates in the TCA cycle (**Fig. 3C**).

Next, our attention turned to whether proteasome inhibition decreases de novo protein synthesis in root tissue. Protein synthesis was estimated by optimizing the nonradioactive SUnSET technique in *B. napus* roots (**Supplementary Fig. S1**). Proteasome inhibition adversely affected protein synthesis at all time points (**Fig. 4**). The effects of MG132 were most severe in

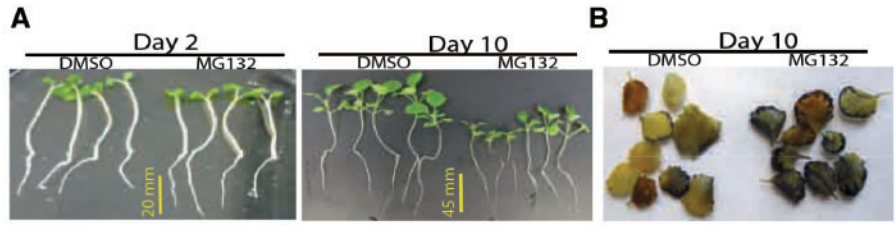

Fig. 1 *Brassica napus* seedlings treated with the proteasome inhibitor MG132 (50 μM) display altered development. (a) Seeds were germinated on vertical media plates containing Hoagland's media and after 5 d were transferred to liquid Hoagland's media. After 2 d of growth in hydroponic media, plants ($n = 25–30$) were transferred to 10 ml of liquid media containing 0.1% DMSO with or without 50 μM MG132. Images are representative of 20–25 different roots from 10 different plants and two experimental replicates. (b) On day 10, starch was visualized upon reaction with 3% Lugol's solution.

Table 1 Proteasome-inhibited plants display altered development.

	Day 0	Day 2		Day 10	
	Control	DMSO	MG132	DMSO	MG132
Total length (mm)	51 (2.2)^a	59 (1.8)^b	57 (3.3)^b	108 (9.1)^c	81 (6.7)^d
Root length (mm)	15 (1.9)^a	20 (1.5)^b	25 (2.2)^c	57 (4.2)^d	45 (4.1)^e
Hypocotyl length (mm)	30 (2.2)^a	39 (2.2)^b	32 (2.1)^a	51 (6.2)^c	36 (5.2)^b
Total weight (mg)	57 (3.7)^a	72 (4.1)^b	69 (5.1)^b	242 (21)^c	111 (14)^d
Chlorophyll (mg/g FW)	NA	NA	NA	9.8 (0.5)^a	10.4 (0.5)^a
Fv/Fm	NA	NA	NA	81.1 (0.1)^a	80.0 (0.2)^b
Starch (mg/g FW)	NA	NA	NA	0.34 (0.1)^a	0.65 (0.1)^b

Root length, hypocotyl length and mass were measured on days 0, 2 and 10 of MG132 treatment. Chlorophyll, Fv/Fm and starch were measured on day 10. Data are the mean and SD of 20–25 seedlings. Different lowercase letters represent a significant difference between treatments ($P < 0.05$).

NA, not available.

plants treated with MG132 for 3 h, when levels of newly synthesized proteins were almost negligible (7%) compared to untreated plants. Protein synthesis after 8 and 48 h of proteasome inhibition was greater compared to 3 h of MG132 treatment, but levels of newly synthesized proteins were not fully restored compared to untreated control plants.

Proteasome inhibition increases de novo amino acid synthesis but did not affect respiration or ROS levels

As described above, proteasome inhibition led to an unexpected increase in glutamine and arginine after 48 h of proteasome inhibition. We reasoned that proteasome inhibition might necessitate adjustments to nitrogen metabolism to support de novo amino acid synthesis. To gain insight into whether nitrogen metabolism is altered, we analyzed the effect of MG132 on NR, which is the first and rate-limiting enzyme in the nitrogen assimilation pathway. MG132 treatment increased the activity of NR after 3 and 8 h but later decreased at 48 h (**Fig. 5A**). We also observed an increase in glutamine synthetase activity 8 h after MG132 treatment (**Fig. 5B**). Because nitrogen and sulfur metabolism are coordinated, we measured protein levels of sulfite reductase (SiR). This enzyme participates in the sulfur assimilation pathways, and we observed increased levels of SiR at all time points (**Fig. 5C**).

We hypothesized that elevated NR activity and levels of SiR could increase the synthesis of amino acids. To answer this question, we examined if MG132 results in an isotopic enrichment of ^{15}N incorporated into newly synthesized amino acids. Proteasome inhibition at 48 h resulted in an overall increase in de novo amino acids (**Fig. 6A** and **Supplementary Table 2**). Most notably, MG132 treatment increased the biosynthesis of glutamine 3-fold compared to control plants after 48 h. The total concentration of amino acids derived from ^{14}N and ^{15}N was calculated to estimate the catabolic and anabolic processes contributing to the levels of free amino acids. After MG132 treatment for 8 and 48 h, amino acids derived from catabolic processes decreased, demonstrating that plant proteasomes contribute to the pool of amino acids derived from catabolic processes. In contrast, after 48 h of proteasome inhibition, the proportion of newly synthesized amino acids doubled compared to control plants (**Fig. 6B** and **Supplementary Table 2**).

Oxygen consumption was measured in the roots of MG132-treated plants to determine if increased amino acid biosynthesis was concomitant with increased respiration to support higher metabolic activity. However, we did not observe any evidence of increased oxygen consumption. In fact, oxygen consumption decreased 3 h after proteasome inhibition (**Fig. 7A**). Decreased rates of respiration were associated with a decrease in the ATP pool after 3 and 8 h of MG132 treatment (**Fig. 7B**). Both ATP and oxygen consumption returned to a homeostatic level at 48 h. We measured levels of COX2—a subunit of the terminal cytochrome C oxidase—to rule out that decreased ATP and oxygen consumption were caused by its decreased abundance. As expected, MG132 did not alter the levels of the COX2 polypeptide (**Fig. 7C**). Intriguingly, proteasome inhibition increased levels of the mitochondrial alternative oxidase (AOX1) at all time points.

AOX1 can be induced by superoxide (Cvetkovska and Vanlerberghe 2013), and we therefore sought to determine if proteasome inhibition induces an accumulation of ROS in intact root tissue. MG132 treatment for 3, 8 and 48 h did not result in increased fluorescence of CellROX, a cell-permeable fluorescent probe that is indicative of ROS (**Fig. 8A**). However, increased fluorescence of Cell ROX was observed in plants treated with cadmium, which is a well-known inducer of ROS and thus served as a warranted positive control given the negligible fluorescence in DMSO and MG132-treated plants. In

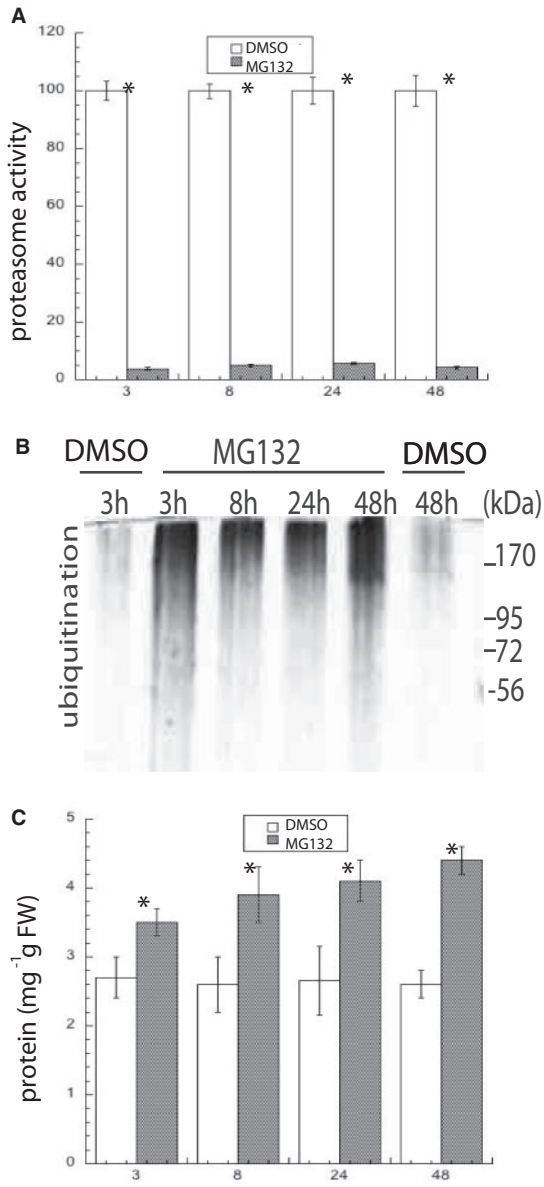

Fig. 2 MG132 impairs the proteasome in *B. napus* seedlings. (A) The chymotrypsin activity of proteasomes was measured in control and MG132-treated plants ($n = 7$) and reported as relative to control plants treated with DMSO at each time point. (B) Ubiquitinated proteins accumulate in MG132-treated plants. Root protein (50 μg) from plants treated with or without MG132 dissolved in DMSO was separated on an 8% SDS–PAGE gel, and ubiquitinated proteins were detected using anti-ubiquitin antiserum. (C) Protein concentration in root tissue was estimated using the Bradford method, and the data represent the mean and SD of seven individual plants. Asterisks represent a significant difference between treatments at each time point ($P < 0.05$). Data are representative for three experimental replicates.

addition, MG132 treatment did not increase the level of superoxide, as judged from NBT staining (**Fig. 8B**).

MG132 induces transcriptional response

Transcriptional reprogramming in response to 8 h of proteasome inhibition in *B. napus* roots was examined using custom-made Affymetrix Brassica exon array chips (BrasEx1Ss520752F) as previously described (Love et al. 2010). Principle component analysis (PCA) of differentially regulated transcripts separated untreated and MG132-treated plants into two distinct groups (**Supplementary Fig. S2**). Using a *P*-value with the FDR of <0.05 and a minimal fold change (FC) of >2 or <-2, a total of 883 transcripts were identified as being differentially regulated when treated with MG132. Of this set, 639 transcripts had an FC of >2 and 244 had an FC of <-2. Among the 639 upregulated transcripts, 470 transcripts were putatively annotated based on predicted Arabidopsis homology (**Supplementary Table S3**). Gene annotations for 174 of the 244 identified downregulated transcripts were assigned. The results of the microarray were validated by performing qPCR analysis on several differentially expressed genes. Results from the qPCR mirror the general trend the transcriptome dataset (**Supplementary Table S4**).

Identified transcripts assigned to a gene ontology (GO) biological process were analyzed to see if they were overrepresented among the up- and downregulated datasets. Overrepresented GO terms were identified in BiNGO using a hypergeometric test after a Benjamini–Hochberg false discovery rate correction. Among the dataset containing genes upregulated by MG132, there was an enrichment of transcripts responsive to abiotic stress and stimuli (**Table 2**). Perhaps most noteworthy was an enrichment of transcripts responsive to abscisic acid; the frequency of transcripts associated with this GO term was 4-fold higher compared to the expected frequency of the Arabidopsis genome.

A manual analysis of upregulated transcripts (**Supplementary Table S3**) identified five transcripts involved in amino acid synthesis, including the synthesis of asparagine, proline, serine and branched-chain amino acids. SiR was upregulated 4-fold and corresponds to the observed accumulation of this protein. Lastly, 11 transcripts were identified that were involved in proteolysis; these include PAA2—a subunit of the 20S proteasome—and the mitochondrial protease FTSH10. Notably, PAA2 and FTSH10 were upregulated 28- and 93-fold, respectively.

Among the identified transcripts that were downregulated by proteasome inhibition, overrepresentation of GO terms includes genes whose biological function pertains to catalytic activity, catalytic process, generation of precursor metabolites and energy and multicellular organismal development. In addition, the frequency of downregulated transcripts involved in glycolysis was overrepresented 35-fold compared to the expected frequency in Arabidopsis.

Discussion

The response to proteasome inhibition in plants is distinct compared to heterotrophs but shares similarities with TOR inhibition

We report that nonlethal proteasome inhibition results in broad metabolic dysregulation in *B. napus* roots. Lethality in proteasome-inhibited yeast, drosophila and human cells is attributed to the depletion of amino acids (Suraweera et al. 2012). A previous study in MG132-treated Arabidopsis roots noted a decrease in protein synthesis and free amino acids after 16 h of MG132 treatment (Van Hoewyk 2016). In our study,

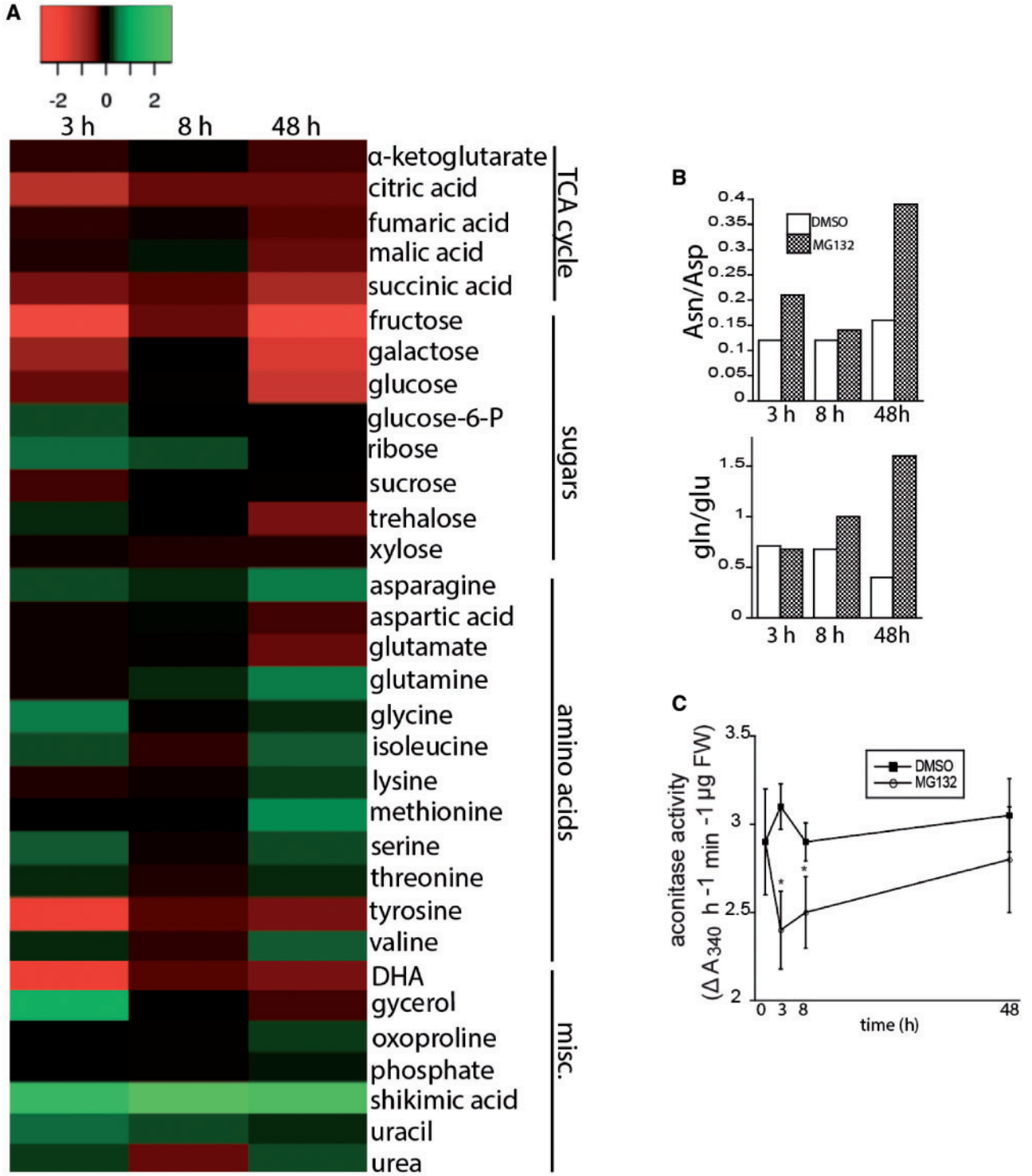

Fig. 3 Proteasome inhibition reconfigures metabolites in the root tissue of *B. napus*. (A) The heatmap highlights the effects of MG132 treatment at 3, 8 and 48 h compared to untreated samples at each time point. Each box represents the mean log2 FC in proteasome-inhibited plants ($n = 4$) relative to untreated plants. (B) Gln/Glu and Asn/Asp peak ratios. (C) Aconitase activity was measured in the root tissue of plants treated with 0.1% DMSO containing or not containing MG132. Data represent the mean and SD from five different plants and are representative of two other experimental replicates. Asterisks represent a significant difference between treatments at each time point ($P < 0.05$). Nd, not detected.

levels of free amino acids declined after 8 h of proteasome inhibition but then were restored after 48 h. Although the same concentration of MG132 was used in both studies, the discrepancy in free amino acids between the two species might reflect decreased potency in *B. napus*, which has much greater biomass compared to Arabidopsis.

Although Svozil et al. (2015) speculated that proteasome inhibition might induce the nitrogen assimilation pathway,

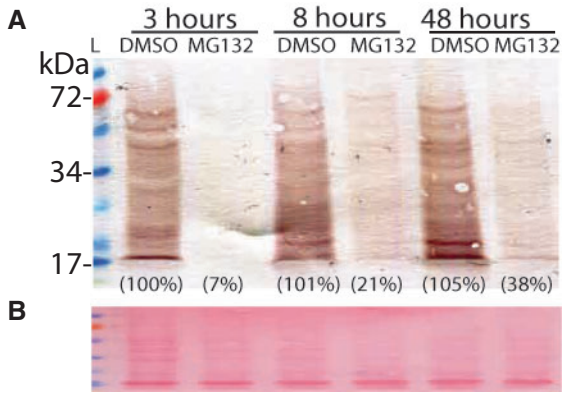

Fig. 4 Proteasome inhibition decreases de novo protein synthesis. Twenty micrograms of root protein from plants treated with or without MG132 were separated on a 10% SDS–PAGE. (A) Immunoreactive bands represent newly synthesized proteins using the SUnSET technique. Numbers depict the mean band intensity of MG132-treated plants relative to untreated plants at each time point ($n = 3$ experimental replicates). (*B*) Ponceau red staining of identical protein samples on a separate gel. L, ladder.

our study was the first to experimentally demonstrate this. As expected, proteasome inhibition decreased free amino acids derived from proteasomal proteolysis, but this was offset by increasing NR activity that supported downstream amino acid synthesis. NR activity increased at 3 and 8 h, which was possibly induced by a sudden decrease in glutamine immediately after MG132 application; whether nitrate reduction and assimilation are directly or indirectly stimulated by proteasome inhibition is not clear. NR decreased activity at 48 h and reflects negative feedback caused by glutamine accumulation.

Decreased protein synthesis is a global response during proteasome inhibition in plants (Cai et al. 2018) and mammals (Bush et al. 1997, Ding et al. 2006). Curiously, decreased protein synthesis during proteasome inhibition cannot completely be explained by a depletion in amino acids. Although protein overload might suppress proteins synthesis until damaged proteins are cleared or repaired, it also cannot fully account for decreased protein synthesis; this conclusion is made because protein concentration and synthesis increase at 48 h in MG132-treated plants compared to earlier time points. Protein synthesis is energetically expensive, and it is possible that the sharp decline in de novo proteins 3 h after MG132 application reflects ATP depletion at the same time point.

In MG132-treated plants, a partial recovery of protein synthesis at 48 h coincided with increased ATP and amino acid synthesis compared to earlier time points and not reduced efficacy of the inhibitor. The ability of plants to increase amino acid synthesis and maintain the amino acid pool in response to proteasome inhibition might be unique compared to heterotrophic organisms and serve to offset the toxicity of proteasome inhibition in plants, as depicted in our model (Fig. 9). Comparing proteasome-induced lethality between autotrophs and heterotrophs supports this possibility. Viability (but not cell count) was unaltered in Chlamydomonas cells treated with 50 μM MG132 for 48 h

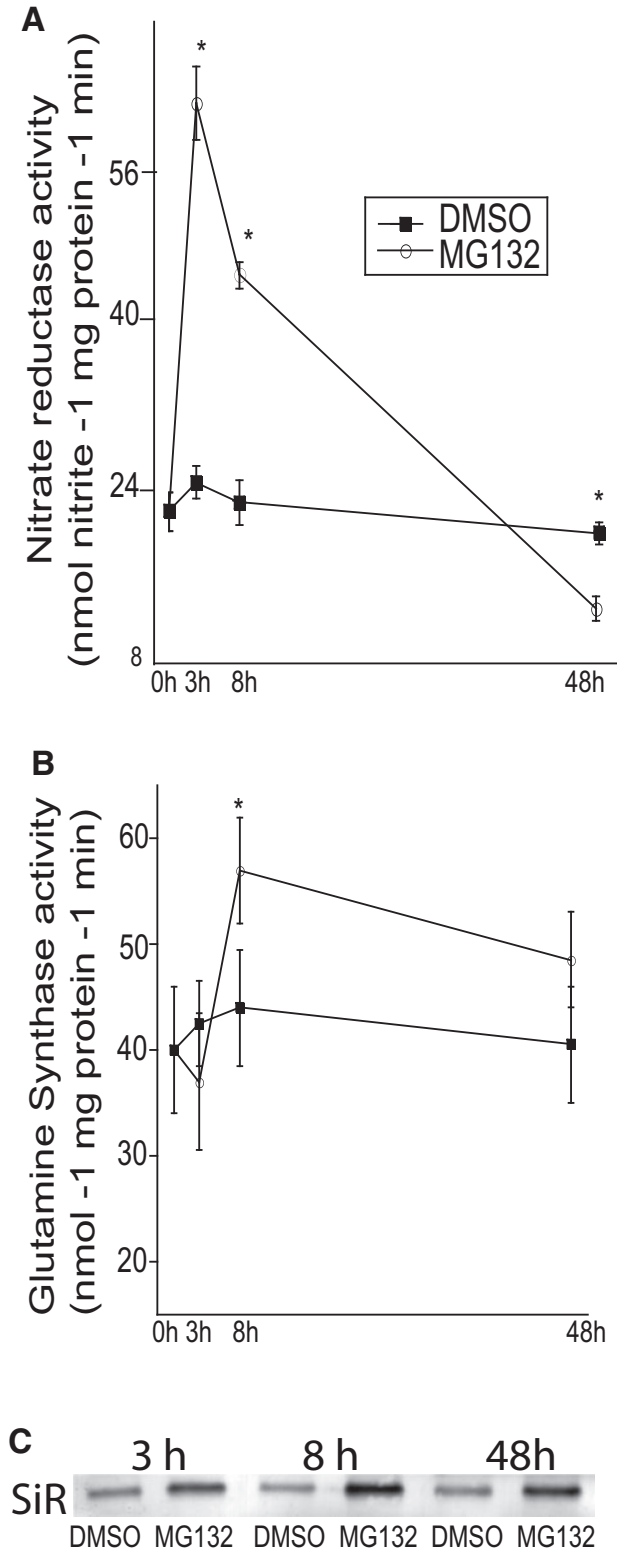

Fig. 5 Proteasome inhibition induces the nitrogen assimilation pathway at early time points. (A) NR and (B) glutamine synthetase activities were measured in roots from plants treated with 0.1% DMSO containing or not containing MG132. Shown are the mean and SD from five different plants. Asterisks represent a significant difference between treatments at each time point ($P < 0.05$). (C) SiR was detected on a 10% SDS–PAGE gels and is representative of two other experimental replicates.

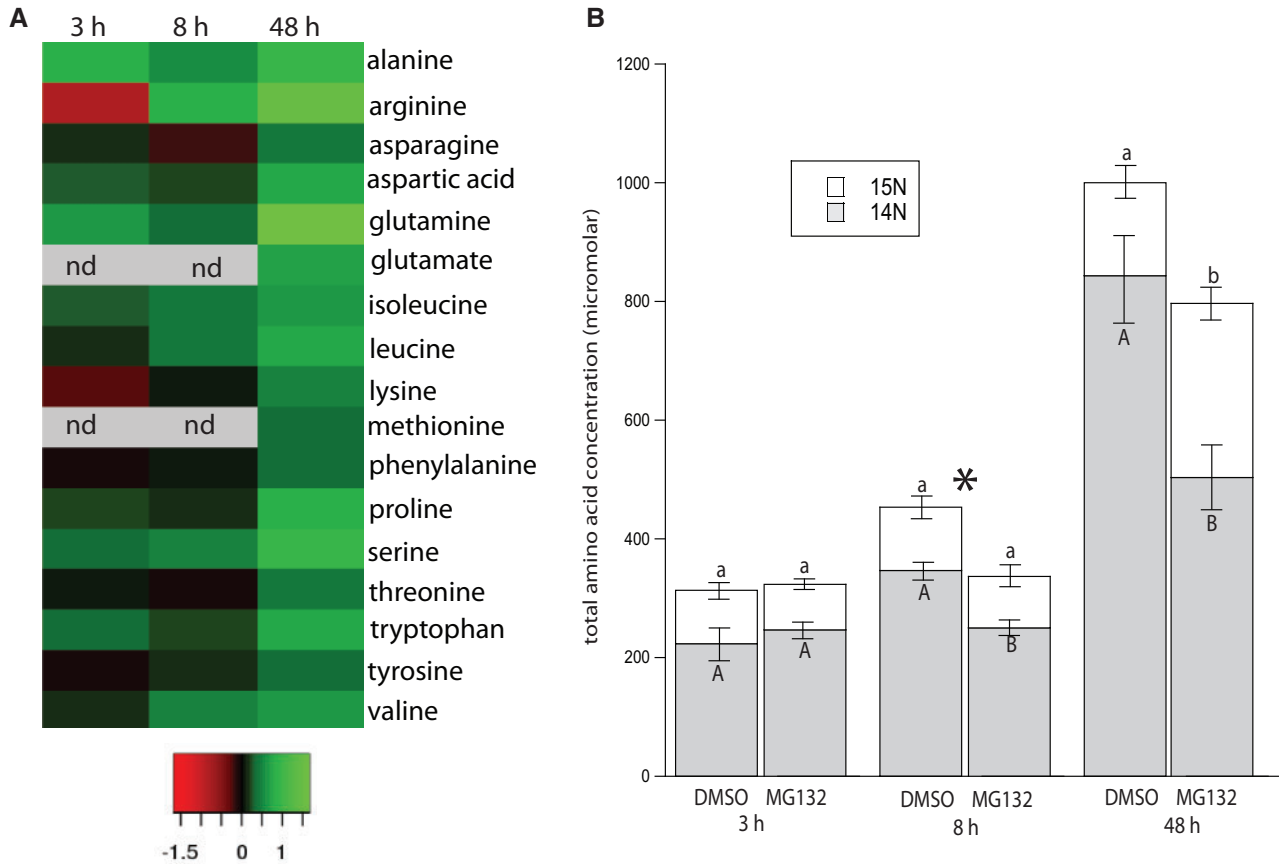

Fig. 6 Proteasome inhibition increases the synthesis of amino acids after 48 h. (A) De novo amino acid synthesis was estimated as the ^{15}N enrichment of amino acids in roots treated with or without MG132 dissolved in 0.1% DMSO. The data represent the log2 FC of isotopic enrichment and SE of each amino acid in MG132-treated plants relative to untreated plants at 3, 8 and 48 h. (B) The free amino acids derived containing ^{14}N and ^{15}N were used to estimate the concentration of amino acids derived from catabolic and anabolic pathways. Shown are the mean and SE of four plant replicates. Different lowercase and uppercase letters represent significant differences ($P < 0.05$) in ^{15}N and ^{14}N amino acids, respectively, between treatments at each time point. The asterisk denotes a significant difference in the free amino acid pool between treatments at each time point. ND, not detected.

(Mendoza et al. 2020). In contrast, 10 μM MG132 reduced viability in mammalian cells to 10% after 8 h compared to untreated cells (Suraweera et al. 2012). The increased potency of proteasome inhibition is also apparent in multicellular autotrophs; proteasome inhibition in Drosophila reduced viability to 25% after 4 d, but *B. napus* in our study appears viable 10 d after MG132 treatment.

The data presented in our study are strikingly similar to the recently reported metabolic adjustments made in TOR-inhibited *Chlamydomonas*. TOR promotes growth and protein synthesis, but its inhibition also decreased TCA cycle metabolites but stimulated nitrogen uptake and assimilation to support elevated rates of amino acid synthesis (Mubeen et al. 2018). Protein synthesis or organismal growth requires both proteasome and TOR homeostasis, but it is not known if plants share a conserved signaling pathway in response to their inhibition.

Abiotic stress can impair plant proteasomes and shares a similar metabolic response to MG132 treatment

As previously mentioned, severe stress decreases proteasome activity. Although a precise mechanism has yet to delineate why stress impairs plant proteasomes, evidence implicates ROS accumulation, which damages subunits of the 19S regulatory particles in mammalian cells (Zmijewski et al. 2009; Shang and Taylor, 2011). Recently, superoxide accumulation induced by severe selenite stress decreased proteasome activity in *Chlamydomonas* (Vallentine et al. 2014) and *B. napus* roots (Dimkovikj and Van Hoewyk 2014).

We observe similarities in the metabolic response of plants treated with MG132 and stressors that induce abiotic stress. For example, oxidative stress is known to decrease protein synthesis (Shenton et al. 2006); salt and MG132 can suppress newly formed proteins to nearly identical levels in Arabidopsis (Van Hoewyk 2016).

We observed the induction of AOX1 and decreased TCA cycle metabolites, which may be an overlapping signature of proteasome inhibition and oxidative stress in root tissue. AOX1 transcripts have previously been reported to increase in response to MG132 (Goda et al. 2008) and oxidative stress (Cvetkovska and Vanlerberghe 2013). In addition, AOX1 is induced by decreased aconitase activity and metabolic perturbation (Sieger et al. 2005), which we observed in our study. In another study, menadione-induced ROS accumulation in

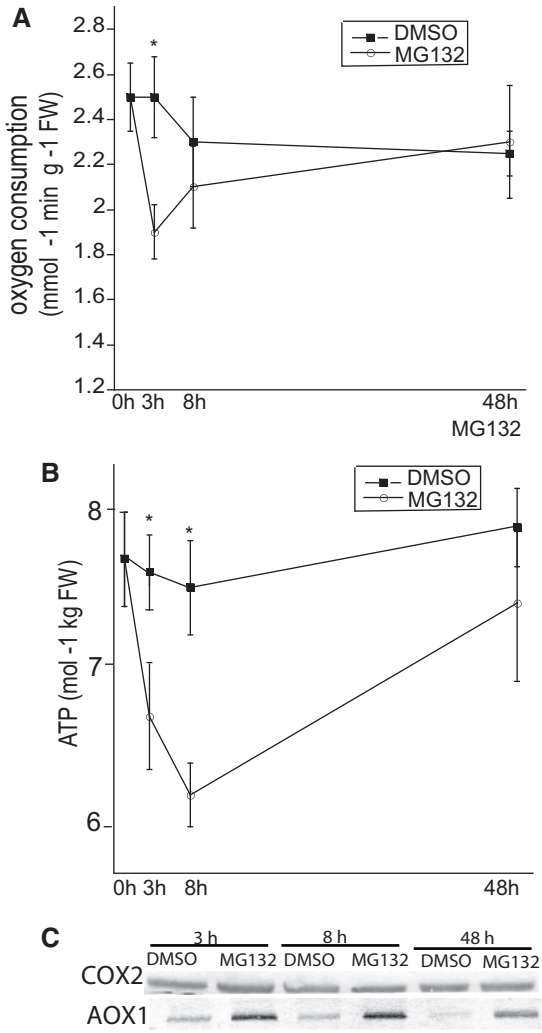

Fig. 7 Proteasome inhibition decreases respiration and ATP levels but recovers after 48 h. (A) Oxygen consumption and (B) ATP levels in roots of plants treated with or without MG132 for 3, 8 and 48 h. Shown are the mean of six individual plants and SD. Asterisks represent a significant difference between treatments at each time point ($P < 0.05$). (C) Levels of the subunit Cox2 and AOX1 were detected on a 10% SDS–PAGE and represent three experimental replicates.

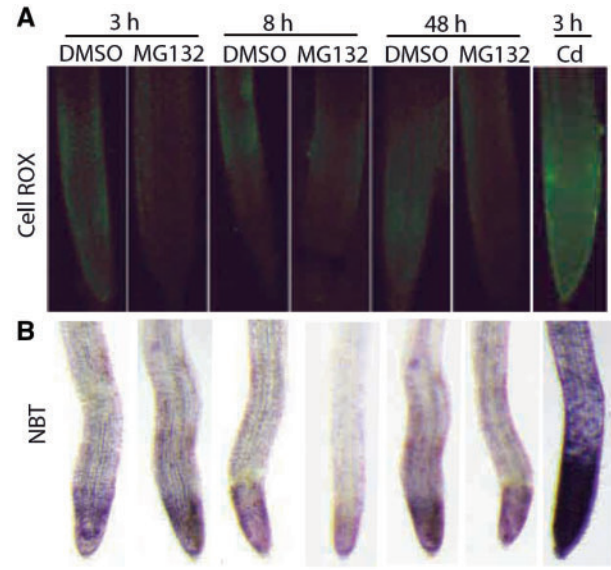

Fig. 8 Proteasome inhibition does not induce ROS accumulation. *Brassica napus* plants were treated with or without 50 μM MG132 dissolved in 0.1% DMSO for the time indicated prior to root excision and incubation with the fluorescent probe Cell ROX (A) and NBT (B). Epifluorescence is representative of 20–25 root tips from 10 different plants and 2 experimental replicates.

Arabidopsis decreased TCA cycle metabolites and the amino acids aspartate and glutamate but increased levels of most amino acids including glutamine and asparagine (Lehmann et al. 2009); these results mirror observations in our study. Identical observations were made in another study examining the impact of selenite-induced oxidative stress on the metabolism in *B. napus*; in that study, decreased proteasome activity also coincided with decreased TCA cycle intermediates, AOX1 induction and the accumulation of amino acids (Dimkovikj and Van Hoewyk 2014).

Lastly, proteasome inhibition resulted in the accumulation of starch in the leaves of developing seedlings. Similarly, starch has also been observed to accumulate in leaves during N starvation (Yu et al. 2017) and altered abscisic acid signaling (Wang et al. 2017). Starch accumulation in the leaves of MG132-treated plants likely stemmed from decreased demand for sugars from source to sink tissues. This conclusion coincides with a decrease in aconitase activity and a repression of transcripts involved in catabolic processes and sugar utilization in roots.

Proteasome inhibition points to perturbed abscisic acid signaling but did not increase ROS

Proteasome inhibition in Arabidopsis results in hypersensitivity to abscisic acid. Our transcriptome analysis further evinced a perceived abscisic acid imbalance, which is reminiscent of the transcriptional response in Arabidopsis plants with a mutation in RIFP1, an E3 ligase that targets an abscisic acid receptor (Li et al. 2016). *Pseudomonas* infection in plants alters abscisic acid signaling (de Torres-Zabala et al. 2007) and increases levels of amino acids (Ward et al. 2010); these phenomena (also observed in our study) can be attributed to *Pseudomonas* effector molecules that inhibit the proteasome and promote pathogenesis. A coordinated stress response requires abscisic acid, which is mediated by the proteasomal removal of the transcriptional factor ABI5 (Han et al. 2018). In addition, proteasomes are well-known to govern levels and proper signaling of other hormones, e.g. ethylene, gibberellin, salicylic acid and auxin (Santner and Estelle 2009). Therefore, if severe pathogenic effectors or abiotic stress inhibits the proteasome, it will likely interfere with hormonal homeostasis that necessitates proper plant development and adjustments to stress (**Fig. 9**).

Notably, proteasome inhibition did not result in ROS accumulation at the time points measured. This is in contrast to the ROS accumulation induced by proteasome

Table 2 Enrichment of GO terms in plants treated with MG132 for 8 h

GO term	GO group	*P*-value	Corrected *P*-vale	Cluster frequency	Total frequency
Enrichment of upregulated transcripts assigned a GO term					
Response to abiotic stimuli	9,628	3.69E−04	3.47E−02	36/463 7.7%	1,168/27,594 4.2%
Postembryonic development	9,791	5.17E−04	4.86E−02	29/463 6.2%	884/27,594 3.2%
Reproduction	3	5.57E−04	1.00E−02	30/463 6.4%	931/27,594 3.3%
Response to stress	6,950	6.41E−04	1.00E−02	50/463 10.7%	1,853/27,594 6.7%
Cellular response to ABA	71,215	7.98E−04	1.00E−02	17/463 3.80%	275/30,320 0.9%
Enrichment of downregulated transcripts assigned a GO term					
Glycolysis	6,096	5.36E−06	2.66E−03	5/169 3.5%	40/27,594 0.1%
Smallmolecular catabolic process	44,282	1.00E−05	2.66E−03	8/169 5.6%	163/27,594 0.7%
Catabolic process	9,056	2.27E−04	4.64E−03	13/169 7.6%	660/27,594 2.3%
Multicellular organismal development	7,275	1.24E−03	1.27E−02	21/169 12.4%	1,655/27,594 5.9%
Generationof precursor metabolites and energy	6,091	1.46E−03	1.33E−02	6/169 3.5%	199/27,594 0.7%
Catalytic activity	3,824	3.10E−03	2.54E−02	63/169 37.2%	7,553/27,594 27.3%

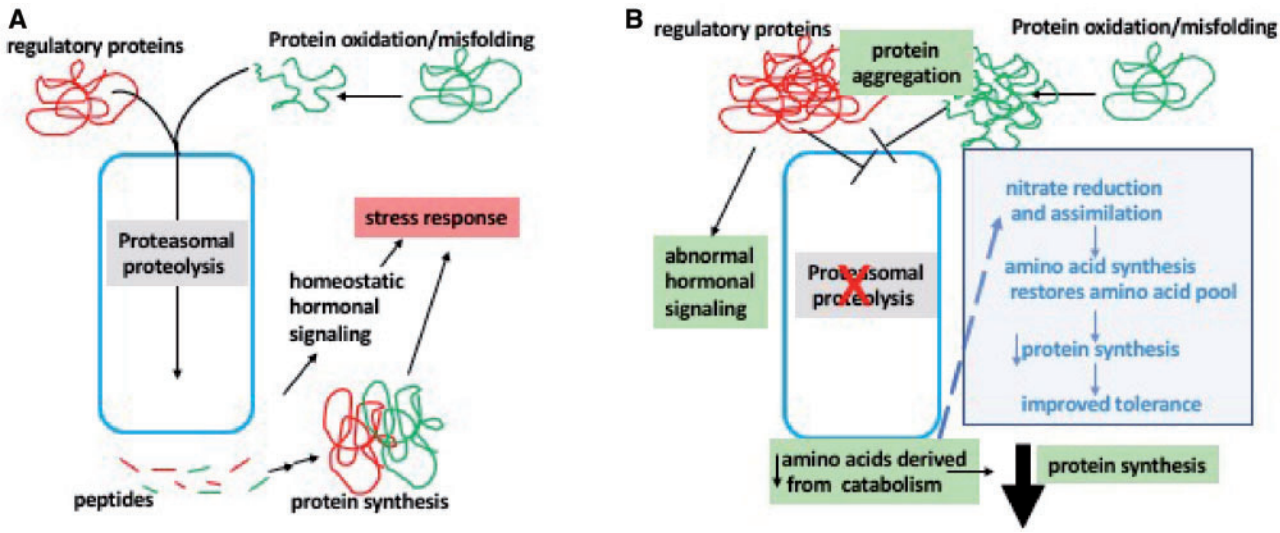

Fig. 9 Schematic diagram of proteasome inhibition in plants. During mild stress (A), proteasomes remove regulatory proteins and damaged proteins to help mediate tolerance to stress. Pathogen effectors and ROS during severe stress (B) can reduce proteasome activity and restrict plant development (green box) by altering hormone signaling, increase protein aggregation and decrease protein synthesis. Proteasome inhibition directly or indirectly induces nitrogen assimilation (blue dotted line). The resulting de novo amino acids might partially ameliorate protein synthesis impairment, leading to improved stress tolerance stemming from proteasome inhibition (blue box).

inhibition that has been reported in pollen tubes (Vannini et al. 2014) and Arabidopsis protoplasts (Kim et al. 2003). Our study did not investigate whether prolonged proteasome inhibition causes oxidative stress in plants. Because proteasome inhibition perturbs metabolism and hormonal signaling, it is likely that extended MG132 treatment would have downstream effects including ROS accumulation.

Future considerations: does proteasome activity underpin stress tolerance?

Proteasomes are required for an effective stress response but are impaired during severe stress. For example, severe selenium stress in *Chlamydomonas* impaired proteasome activity, which prevented the removal of nonspecific and misfolded selenoproteins, and therefore sensitized the cells to selenium (Vallentine et al. 2014). Our data show that the response to MG132 treatment resembles metabolic adjustments made during abiotic stress; thus, minimizing proteasome impairment during stress should improve plant performance (Fig. 9). In support of this idea, a recent QTL study identified an allele encoding a subunit of the 20S proteasome that confers thermotolerance in a rice ecotype (Li et al. 2016); the allele also confers heat tolerance in transgenic Arabidopsis, which was explained by the observed increase in proteasome activity. Given the proteasome's role in plant hormone signaling, development and metabolic poise observed in this study, maintenance of proteasome activity during stress could provide plants with enhanced tolerance to environmental constraints.

PCP PLANT & CELL PHYSIOLOGY

Materials and Methods

Growth conditions and initial stress-induced measurements

Brassica napus seeds were germinated in a growth chamber (250 μmol m^{-2} s^{-1} PAR, 14-h light/10-h dark cycle, 24°C) on vertical agar plates containing Hoagland's media; after 5 d, seedlings were transferred to 1 l of aerated liquid Hoaglandoa media. Initial stress measurements were measured in seedlings to determine the toxic effects of 50 μm MG132, as described (**Fig. 1**). All other experiments were performed in 4-week-old plants growing in 2 l of liquid media, which was changed every 5-7 d. To induce proteasome inhibition, plants ($n = 30–40$) were transferred into 250 ml of media ± MG132 as similarly described above. After 24 h, media were replenished. For all remaining experiments, unless otherwise described, root tissue was harvested from individual plants at 0, 3, 8 and 48 h.

Microscopy

The cell-permeable fluorescent probe CellRox Green (Invitrogen) was used to visualize ROS at 3, 8 and 48 h in the roots of plants treated ± MG132. Root tips ($n = 30$) were excised (10–12 mm) and placed in 1 ml of buffer containing 50 mM Tris, pH 7.5, and 5 μM CellRox Green. Root tips were incubated on a rotating platform in the dark for 30 min and subsequently washed three times in 50 mM Tris, pH 7.5, to remove residual CellRox Green that would otherwise increase background fluorescence. CellRox Green fluoresces optimally at Ex485/Em520 and was observed using an FITC filter.

Protein electrophoresis and protein synthesis estimates

Immunoblotting was used to determine the effect of MG132 treatment on various polypeptides in root tissue. Proteins were extracted in 50 mM Tris, pH 7.5, 100 mM NaCl, 0.5% triton-X, 2 mM dithiothreitol and 0.5 mM of the protease inhibitor PMSF and heated for 10 min at 85°C. Unless otherwise stated, 20 μg of denatured protein was separated on reducing SDS–PAGE (10% or 12% acrylamide gels) and transferred to a PVDF membrane by electroblotting. Commercial antibodies for AOX1 and COX2 were obtained from Agrisera. Levels of ubiquitinated proteins were detected on 8% gels containing 50 μg of protein per lane, which reacted against ubiquitin antiserum (Santa Cruz Biotechnology) as previously described (Sabbagh and Van Hoewyk 2012). Protein content was determined using the Bradford method; the absorbance (595 nm) of reactions containing root protein extract was plotted against a standard curve generated using bovine serum albumin.

Protein synthesis was estimated by using the nonradioactive SUnSET method (Schmidt et al. 2009, Van Hoewyk 2016). Briefly, roots were treated with a low concentration of puromycin, which gets incorporated into nascent polypeptides and causes termination. Truncated proteins containing puromycin are then detected by immunoblotting using puromycin antiserum. After DMSO or MG132 treatment, individual plants were immediately transferred to 10 ml of Hoagland's media containing 40 μM puromycin for 25 min. To detect the truncated proteins that arise from puromycin's misincorporation into polypeptides, 20 μg of protein was loaded onto a 15% SDS–PAGE gel and run under denaturing conditions as described above. Prior to immunoblotting, membranes were stained with Ponceau red to ensure an equal loading of proteins between lanes. Membranes were incubated for 2 h with the puromycin antibody (PMY-2A4) purchased from the University of Iowa, USA. The PMY-2A4 antibody was used at a 1:1,000 dilution. Newly synthesized proteins containing puromycin were detected using a secondary antibody conjugated to alkaline phosphatase (1:10,000 dilution for 45 min). Protein synthesis was estimated based on the intensity of immunoreactive bands using ImageJ.

Enzymatic assays

NR activity in roots was performed using a modified procedure by Hageman and Reed (1980). In a 1-ml reaction mixture containing 25 mM potassium phosphate (pH 7.4), 1 mM EDTA, 10 mM potassium nitrate and 0.10 mM NADH, 50 μl of protein extract was added and allowed to react for 5 min at 30°C. The reaction was stopped by adding 0.5 ml of 58 mM of sulfanilamide dissolved in 3 M HCl, followed by 0.5 ml of 0.77 mM 1-naphthyl ethylenediamine dihydrochloride. Mixture incubated for 10 min at room temperature and developed a magenta hue. Absorbance (570 nm) was measured spectrophotometrically, and activity was measured against a standard curve in which protein extract was replaced with purified NR. One unit of activity is the amount of enzyme that generated 1 mmol of NO_2 per min.

The chymotrypsin activity of the proteasome was measured as previously described (Dimkovikj and Van Hoewyk 2014). Briefly, proteins were extracted in proteasome extraction buffer [50 mM potassium phosphate buffer—pH 7.4, 5% (v/v) glycerol, 10 mM ATP, 5 mM beta-mercaptoethanol]. Proteasome activity was measured fluorometrically (Ex360/Em410) containing 5 μl of protein extract and 95 μl of reaction buffer (50 mM potassium phosphate buffer, pH 7.4, 2 mM $MgCl_2$, 1 mM ATP, 5 mM beta-mercaptoethanol) with 50 μM of the fluorogenic peptide Suc-LLVY-AMC in DMSO. The released AMC fluorescence was recorded on a BioTek plate reader. The activity was determined after 60 min as the difference in increased fluorescence in reactions with or without MG132 (20 μM) to account for the non-proteasomal release of AMC. Proteasome activity is expressed as the net changes of fluorescence (RFU min^{-1} μg $protein^{-1}$) in the presence and absence of the proteasome inhibitor MG132.

Aconitase activity was measured in root tissue as previously performed (Dimkovikj and Van Hoewyk 2014) using an aconitase assay kit according to the manufacturer's directions (Cayman Chemical, USA). Briefly, a native protein extract was collected as described above and added to a reaction buffer containing 50 mM Tris, pH 7.4, sodium-citrate, $NADP^+$ and isocitrate dehydrogenase. In this coupled-enzymatic reaction, citrate is isomerized via aconitase into isocitrate, which is then catalyzed by isocitrate dehydrogenase into ketoglutarate and NADPH. Aconitase activity was measured at an absorbance of 340 nm and was proportional to the reduction in NADP to NADPH.

Transcriptome analysis and qPCR validation

To determine how proteasome inhibition altered the transcriptome, plants were grown with or without MG132 for 8 h. mRNA from root tissue (100 mg) was isolated and cleaned using an RNeasy min kit (Qiagen) and subsequently used to synthesize cDNA using Superscript reverse transcriptase (Invitrogen) according to the manufacturer's instructions, as performed similarly (Van Hoewyk et al. 2008). Integrity and purity of cDNA were confirmed using a Bioanalyzer (Agilent Technologies) and then hybridized onto a custom-made Affymetrix Brassica Exon array chip containing over 135,000 unique gene sets as first described (Love et al. 2010). Data analysis was conducted in Partek Genomics Suite; this included PCA to determine if gene expression differed among the two treatments (three replicates). Differentially regulated transcripts caused by MG132 were identified as probe sets with an FC of >2 or <-2 compared to untreated samples and a *P*-value and FDR of <0.05. Probe sets were assigned a Brassica gene ID, and the biological function of each gene was putatively annotated if gene contained an Arabidopsis homolog. Identified transcripts assigned to a GO biological process were analyzed to determine if they were overrepresented among the up- and downregulated datasets. Overrepresented GO terms were identified in BiNGO using a hypergeometric test after a Benjamini–Hochberg false discovery rate correction.

Several identified genes were selected for qRT-PCR analysis to validate the microarray dataset. cDNA was synthesized as performed for the microarray array experiment from three separate experimental replicates. Primer pairs were designed using Primer3, and their specificity against their targeted genes was validated using BLAST; the sequence of primers is provided. qPCR amplifications and data analysis were performed on a CFX PCR Detection System (BioRad) according to the manufacturer's instructions. Briefly, the 10-μl reaction contained 3 μl of diluted cDNA (1:100), 1 μl of each forward and reverse primer and 5 μl of SsoAdvanced SYBR Green Supermix (BioRad). Treatments were analyzed as three biological replicates, each containing three technical replicates. The PCR cycling conditions were: 95°C for 30 s, 35 cycles of 95°C for 10 s, 60°C for 10 s, followed by a melting curve analysis from 65°C to 95°C. The $2-\Delta\Delta$Ct method was used to calculate the relative expression of the target genes (Livak and Schmittgen 2001). PPA2 and ACT2 were selected as reference genes (Wang et al. 2014), both of which displayed nearly identical amplification efficiency as the selected genes. Transcript expression in MG132-treated samples is expressed as FC relative to control samples using the PPA2 reference gene, and values were similar when using the ACT2 reference gene. A Student's *t*-test

evaluated if there was a significant difference in expression between the two treatments.

Metabolite analysis

A targeted metabolite analysis was performed in plant roots treated with or without MG132 to gauge how proteasome inhibition affects levels of amino acids, sugars and TCA intermediates. Root tissue (75 mg) from four separate plants was ground in liquid nitrogen, extracted in 1 ml of methanol by sonication and centrifuged. The supernatant (750 μl) was transferred into a glass tube, to which 1 ml of chloroform was added. The mixture was placed in an ice bath and 750 μl of cold water was subsequently added to induce the separation of chloroform from the water–methanol phase. After brief centrifugation, 200 µl of the aqueous methanol phase was transferred to vials with glass inserts (250 µl) and dried completely under nitrogen. Five microliters of ribitol in methanol (500 µg ml^{-1}) and 5 µl of d^{27}-myristic acid in hexane (1 mg ml^{-1}) were added to each vial and dried completely under nitrogen. The samples were methoxylaminated via reaction with 20 µl of methoxylamine hydrochloride (20 mg ml^{-1}) in pyridine at 40°C for 90 min. Furthermore, the acidic protons in the compounds were silylated via reaction with 80 μl of *N*-methyl-*N*-(trimethylsilyl) trifluoroacetamide with 1% trimethylchlorosilane for 40 min at 40°C. The samples were analyzed using gas chromatography–mass spectrometry (GC–MS) within 10 h of derivatization.

The samples were analyzed using an Agilent 7980A GC system coupled with a 5975 C series mass detector and separation of metabolites was achieved on a DB-5 MS capillary column (30 m length × 0.25 mm internal diameter × 0.20 µm film thickness) with a 1:10 split of a 1 µl injection. The temperature program of the GC was as follows: 60°C for 1 min, followed by a temperature ramp of 10°C per minute to 315°C, with a 10-min hold at 315°C prior to re-equilibration at 60°C. The carrier gas (He) was maintained at a constant pressure of 10.7 psi; the injection port and the MS interphase were maintained at 270°C; the MS quad temperature was maintained at 150°C; and the MS source temperature was set at 240°C. The electron multiplier was operated at a constant gain of 2 (EMV = 1,705 V) and the scanning range was set at 50–600 amu, achieving 2.66 scans s^{-1}. The mass spectra were further processed using the Automatic Mass Spectral Deconvolution and Identification System (v2.71, NIST) with the following deconvolution parameters: match factor—75%; resolution—high; sensitivity—medium; and shape requirements—medium. The compounds were positively identified based on an in-house retention index mass spectral library supplemented with Fiehn Lib (G1676AA; Agilent Technologies, Wilmington, DE, USA), which contains the retention indices and mass fragment information for 768 plant metabolites, and the NIST11 mass spectral library. All positive matches were confirmed by manual curation, and the integrated area with reference to internal standard was used for further statistical analysis. The extractable polar metabolites were grouped into amino acids, organic acids, phenolic acids, sugars and sugar alcohols for statistical analyses. Data were normalized to the internal standard ribitol and are reported as relative levels to DMSO-treated control plants.

Enrichment of ^{15}N to determine de novo amino acid synthesis was conducted as per the procedures described in Maroli et al. (2016). Amino acids were analyzed using a Shimadzu Ultra-Fast liquid chromatography, connected in tandem to an electrospray ionization triple-quadrupole mass spectrometer (Shimadzu 8040). The amino acids were separated on a 100 mm × 3 mm i.d. × 2.6 μm, Kinetex XB-C18 column (Phenomenex, Torrance, CA, USA) using a gradient elution of 0.05% formic acid (solvent A) and methanol (solvent B) at a solvent flow rate of 0.3 ml/min. Solvent B was initially held at 4% for 2 min and was then linearly increased to 16% by 9 min, 46% by 14 min and re-equilibrated at 4% B for 7 min. Tandem mass spectrometry experiments were performed on a triple-quadrupole tandem mass spectrometer. Single-ion transitions (m/z) for each of the ^{14}N and ^{15}N amino acids were optimized using authentic ^{14}N- and ^{15}N-labeled amino acid standards [cell-free amino acid mixture—^{15}N (98 atom % ^{15}N)] (Aldrich Chemicals, Sigma-Aldrich Co., St. Louis, MO, USA). ^{15}N-Amino Acid isotopologue enrichment calculations were done as specified (Maroli et al. 2016).

Levels of ATP in root tissue were estimated using an ATP bioluminescence kit (Promega, USA). ATP was extracted in 1 ml of 3% trichloroacetic acid by grinding tissue (140–160 mg) in liquid nitrogen. After centrifuging (16,000 rpm), 300 μl of supernatant was neutralized in potassium-hydroxide (pH 7.8). ATP was estimated by adding 5 μl of extract into 95 μl of reaction buffer containing luciferase, and luminescence was immediately measured on a Promega Glo-Max Multi Jr luminometer.

Starch and photosynthetic measurements

Starch content was estimated in seven samples, with each sample containing five pooled leaves . Briefly, chlorophyll was removed in detached leaves by heating samples to ∼75°C in 80% ethanol for 15 min. Leaves were subsequently pulverized in liquid nitrogen, boiled for 1 min in 1 ml of water and then allowed to react with a 0.2% Lugol's iodine solution. The starch–iodine complex was measured spectrophotometrically at an absorbance of 630 nm; levels of starch in leaf tissue were estimated using a standard curve containing known starch levels. Starch was visualized in intact leaves by removing chlorophyll as described above and applying a 3% Lugol's solution.

Analysis of chlorophyll levels and chlorophyll fluorescence was performed as previously described (Grant et al. 2011). Total chlorophyll was measured from intact leaves on day 10 by extracting in dimethylformamide and measuring the extract on a spectrophotometer at A_{652}. The efficiency of photosystem II was evaluated by estimating the Fv/Fm values on a handheld chlorophyll fluorometer (Photon System Instruments, Bratislava, Czech Republic) in dark-adapted plants treated with or without MG132 for 10 d.

Oxygen consumption

Oxygen consumption was measured using the Oxygraph Plus system (Hansatech, Norwich, UK). Excised root tissue (100–150 mg) was transferred into an airtight cuvette containing 2 ml of Hoagland's media ± MG132 solution, and oxygen consumption rate was measured using a Clark-type electrode. Oxygen consumption was estimated as the difference in oxygen concentration in the reaction vessel after 15 min. Total respiration is expressed as the concentration of oxygen consumed^{-1} min^{-1} mg fresh weight of root tissue.

Supplementary Data

Supplementary data are available at PCP online.

Funding

The National Science Foundation (MCB1615318) to D.V.H.

Disclosures

The authors have no conflicts of interest to declare.

References

Bence, N.F., Sampat, R.M. and Kopito, R.R. (2001) Impairment of the ubiquitin-proteasome system by protein aggregation. *Science* 292: 1552–1555.

Bush, K.T., Goldberg, A.L. and Nigam, S.K. (1997) Proteasome inhibition leads to a heat-shock response, induction of endoplasmic reticulum chaperones, and thermotolerance. *J. Biol. Chem.* 272: 9086–9092.

Cai, Y.M., Yu, J., Ge, Y., Mironov, A. and Gallois, P. (2018) Two proteases with caspase-3-like activity, cathepsin B and proteasome, antagonistically control ER-stress-induced programmed cell death in Arabidopsis. *New Phytol.* 218: 1143–1155.

Chiu, R.S., Pan, S., Zhao, R. and Gazzarrini, S. (2016) ABA-dependent inhibition of the ubiquitin proteasome system during germination at high temperature in Arabidopsis. *Plant J.* 88: 749–761.

Cvetkovska, M. and Vanlerberghe, G.C. (2013) Alternative oxidase impacts the plant response to biotic stress by influencing the mitochondrial generation of reactive oxygen species. *Plant Cell Environ.* 36: 721–732.

Chung, K.K., Dawson, V.L. and Dawson, T.M. (2001) The role of the ubiquitin-proteasomal pathway in Parkinson's disease and other neurodegenerative disorders. *Trends Neurosci.* 24: 7–14.

de Torres-Zabala, M., Truman, W., Bennett, M.H., Lafforgue, G., Mansfield, J. W., Egea, P.R., et al. (2007) *Pseudomonas syringae* pv. tomato hijacks the Arabidopsis abscisic acid signalling pathway to cause disease. *EMBO J.* 26: 1434–1443.

Dimkovikj, A. and Van Hoewyk, D. (2014) Selenite activates the alternative oxidase pathway and alters primary metabolism in *Brassica napus* roots: evidence of a mitochondrial stress response. *BMC Plant Biol.* 14: 259.

Ding, Q., Dimayuga, E., Markesbery, W.R. and Keller, J.N. (2006) Proteasome inhibition induces reversible impairments in protein synthesis. *FASEB J.* 20: 1055–1063.

Ekholm, S.V. and Reed, S.I. (2000) Regulation of G1 cyclin-dependent kinases in the mammalian cell cycle. *Curr. Opin. Cell Biol.* 12: 676–684.

Finley, D. (2009) Recognition and processing of ubiquitin-protein conjugates by the proteasome. *Annu. Rev. Biochem.* 78: 477–513.

Genschik, P., Criqui, M.C., Parmentier, Y., Derevier, A. and Fleck, J. (1998) Cell cycle-dependent proteolysis in plants: Identification of the destruction box pathway and metaphase arrest produced by the proteasome inhibitor MG132. *Plant Cell* 10: 2063–2075.

Goda, H., Sasaki, E., Akiyama, K., Maruyama-Nakashita, A., Nakabayashi, K., Li, W., et al. (2008) The AtGenExpress hormone and chemical treatment data set: experimental design, data evaluation, model data analysis and data access. *Plant J.* 55: 526–542.

Grant, K., Carey, N.M., Mendoza, M., Schulze, J., Pilon, M., Pilon-Smits, E.A., et al. (2011) Adenosine 5'-phosphosulfate reductase (APR2) mutation in Arabidopsis implicates glutathione deficiency in selenate toxicity. *Biochem. J.* 438: 325–335.

Groll, M., Schellenberg, B., Bachmann, A.S., Archer, C.R., Huber, R., Powell, T. K., et al. (2008) A plant pathogen virulence factor inhibits the eukaryotic proteasome by a novel mechanism. *Nature* 452: 755–758.

Hageman, R.H. and Reed, A.J. (1980) Nitrate reductase from higher plants. *In Methods in Enzymology, Photosynthesis and Nitrogen Fixation*. Edited by San Pietro, A. pp. 270–280. Academic Press, New York.

Han, J.J., Yang, X., Wang, Q., Tang, L., Yu, F., Huang, X., et al. (2019) The β5 subunit is essential for intact 26S proteasome assembly to specifically promote plant autotrophic growth under salt stress. *New Phytol.* 221: 1359–1368.

Karmous, I., Chaoui, A., Jaouani, K., Sheehan, D., El Ferjani, E., Scoccianti, V., et al. (2014) Role of the ubiquitin-proteasome pathway and some peptidases during seed germination and copper stress in bean cotyledons. *Plant Physiol. Biochem.* 76: 77–85.

Kim, M., Ahn, J.W., Jin, U.H., Choi, D., Paek, K.H. and Pai, H.S. (2003) Activation of the programmed cell death pathway by inhibition of proteasome function in plants. *J. Biol. Chem.* 278: 19406–19415.

Kurepa, J., Toh-e, A. and Smalle, J.A. (2008) 26S proteasome regulatory particle mutants have increased oxidative stress tolerance. *Plant J.* 53: 102–114.

Lehmann, M., Schwarzländer, M., Obata, T., Sirikantaramas, S., Burow, M., Olsen, C.E., et al. (2009) The metabolic response of Arabidopsis roots to oxidative stress is distinct from that of heterotrophic cells in culture and highlights a complex relationship between the levels of transcripts, metabolites, and flux. *Mol. Plant* 2: 390–406.

Li, Y., Zhang, L., Li, D., Liu, Z., Wang, J., Li, X., et al. (2016) The Arabidopsis F-box E3 ligase RIFP1 plays a negative role in abscisic acid signalling by facilitating ABA receptor RCAR3 degradation. *Plant Cell Environ.* 39: 571–582.

Ling, Y.H., Liebes, L., Zou, Y. and Perez-Soler, R. (2003) Reactive oxygen species generation and mitochondrial dysfunction in the apoptotic response to Bortezomib, a novel proteasome inhibitor, in human H460 non-small cell lung cancer cells. *J. Biol. Chem.* 278: 33714–33723.

Livak, K.J. and Schmittgen, T.D. (2001) Analysis of relative gene expression data using real-time quantitative PCR and the $2-\Delta\Delta$CT method. *Methods* 25: 402–408.

Love, C.G., Graham, N.S., Lochlainn, S.Ó., Bowen, H.C., May, S.T., White, P.J., et al. (2010) A Brassica exon array for whole-transcript gene expression profiling. *PLoS One* 5: e12812.

Lyzenga, W.J. and Stone, S.L. (2012) Abiotic stress tolerance mediated by protein ubiquitination. *J. Exp. Bot.* 63: 599–616.

Maharjan, S., Oku, M., Tsuda, M., Hoseki, J. and Sakai, Y. (2015) Mitochondrial impairment triggers cytosolic oxidative stress and cell death following proteasome inhibition. *Sci. Rep.* 4: 11.

Maroli, A., Nandula, V., Duke, S. and Tharayil, N. (2016) Stable isotope resolved metabolomics reveals the role of anabolic and catabolic processes in glyphosate-induced amino acid accumulation in *Amaranthus palmeri* biotypes. *J. Agric. Food Chem.* 64: 7040–7048.

Marshall, R.S., Li, F., Gemperline, D.C., Book, A.J. and Vierstra, R.D. (2015) Autophagic degradation of the 26S proteasome is mediated by the dual ATG8/ubiquitin receptor RPN10 in Arabidopsis. *Mol. Cell* 58: 1053–1066.

Mendoza, F., Berry, C., Prestigiacomo, L. and Van Hoewyk, D. (2020) Proteasome inhibition rapidly exacerbates photoinhibition and impedes recovery during high light stress in *Chlamydomonas reinhardtii*. *BMC Plant Biol.* 20: 22.

Mubeen, U., Jüppner, J., Alpers, J., Hincha, D.K. and Giavalisco, P. (2018) Target of rapamycin inhibition in *Chlamydomonas reinhardtii* triggers de novo amino acid synthesis by enhancing nitrogen assimilation. *Plant Cell* 30: 2240–2254.

Pena, L.B., Zawoznik, M.S., Tomaro, M.L. and Gallego, S.M. (2008) Heavy metals effects on proteolytic system in sunflower leaves. *Chemosphere* 72: 741–746.

Sabbagh, M. and Van Hoewyk, D. (2012) Malformed selenoproteins are removed by the ubiquitin-proteasome pathway in *Stanleya pinnata*. *Plant Cell Physiol.* 53: 555–564.

Santner, A. and Estelle, M. (2009) Recent advances and emerging trends in plant hormone signalling. *Nature* 459: 1071–1078.

Schmidt, E.K., Clavarino, G., Ceppi, M. and Pierre, P. (2009) SUnSET, a nonradioactive method to monitor protein synthesis. *Nat. Methods* 6: 275–277.

Schubert, U., Anton, L.C., Gibbs, J., Norbury, C.C., Yewdell, J.W. and Bennink, J.R. (2000) Rapid degradation of a large fraction of newly synthesized proteins by proteasomes. *Nature* 404: 770–774.

Shang, F. and Taylor, A. (2011) Ubiquitin–proteasome pathway and cellular responses to oxidative stress. *Free Radic. Biol. Med.* 51: 5–16.

Sheng, X., Hu, Z., Lü, H., Wang, X., Baluška, F., Šamaj, J., et al. (2006) Roles of the ubiquitin/proteasome pathway in pollen tube growth with emphasis on MG132-induced alterations in ultrastructure, cytoskeleton, and cell wall components. *Plant Physiol.* 141: 1578–1590.

Sheng, X., Wei, Q., Jiang, L., Li, X., Gao, Y. and Wang, L. (2012) Different degree in proteasome malfunction has various effects on root growth possibly through preventing cell division and promoting autophagic vacuolization. *PLoS One* 7: e45673.

Shenton, D., Smirnova, J.B., Selley, J.N., Carroll, K., Hubbard, S.J., Pavitt, G.D., et al. (2006) Global translational responses to oxidative stress impact upon multiple levels of protein synthesis. *J. Biol. Chem.* 281: 29011–29021.

Sieger, S.M., Kristensen, B.K., Robson, C.A., Amirsadeghi, S., Eng, E.W., Abdel-Mesih, A., et al. (2005) The role of alternative oxidase in modulating carbon use efficiency and growth during macronutrient stress in tobacco cells. *J. Exp. Bot.* 56: 1499–1515.

Suraweera, A., Münch, C., Hanssum, A. and Bertolotti, A. (2012) Failure of amino acid homeostasis causes cell death following proteasome inhibition. *Mol. Cell* 48: 242–253.

Svozil, J., Gruissem, W. and Baerenfaller, K. (2015) Proteasome targeting of proteins in Arabidopsis leaf mesophyll, epidermal and vascular tissues. *Front. Plant Sci.* 6: 376.

Valenzuela, C.E., Acevedo-Acevedo, O., Miranda, G.S., Vergara-Barros, P., Holuigue, L., Figueroa, C.R., et al. (2016) Salt stress response triggers activation of the jasmonate signaling pathway leading to inhibition of cell elongation in Arabidopsis primary root. *J. Exp. Bot.* 67: 4209–4220.

Vallentine, P., Hung, C.-Y., Xie, J. and Van Hoewyk, D. (2014) The ubiquitin-proteasome pathway protects *Chlamydomonas reinhardtii* against selenite toxicity, but is impaired as reactive oxygen species accumulate. *AoB Plants* 6: plu062.

Van Hoewyk, D. (2016) Use of the non-radioactive SUnSET method to detect decreased protein synthesis in proteasome inhibited Arabidopsis roots. *Plant Methods* 12: 20.

Van Hoewyk, D., Takahashi, H., Inoue, E., Hess, A., Tamaoki, M. and Pilon-Smits, E.A. (2008) Transcriptome analyses give insights into selenium-stress responses and selenium tolerance mechanisms in Arabidopsis. *Physiol. Plant.* 132: 236–253.

Vannini, C., Bracale, M., Crinelli, R., Marconi, V., Campomenosi, P., Marsoni, M., et al. (2014) Proteomic analysis of MG132-treated germinating pollen reveals expression signatures associated with proteasome inhibition. *PLoS One* 9: e108811.

Vierstra, R.D. (2003) The ubiquitin/26S proteasome pathway, the complex last chapter in the life of many plant proteins. *Trends Plant Sci.* 8: 135–142.

Wang, S., Kurepa, J., Hashimoto, T. and Smalle, J.A. (2011) Salt stress-induced disassembly of Arabidopsis cortical microtubule arrays involves 26S proteasome-dependent degradation of SPIRAL1. *Plant Cell* 23: 3412–3427.

Wang, Z., Chen, Y., Fang, H., Shi, H., Chen, K., Zhang, Z., et al. (2014) Selection of reference genes for quantitative reverse-transcription polymerase chain reaction normalization in *Brassica napus* under various stress conditions. *Mol. Genet. Genomics* 289: 1023–1035.

Ward, J.L., Forcat, S., Beckmann, M., Bennett, M., Miller, S.J., Baker, J.M., et al. (2010) The metabolic transition during disease following infection of Arabidopsis thaliana by *Pseudomonas syringae* pv. tomato. *Plant J.* 63: 443–457.

Yang, P., Fu, H., Walker, J., Papa, C.M., Smalle, J., Ju, Y.-M., et al. (2004) Purification of the Arabidopsis 26 S proteasome biochemical and molecular analyses revealed the presence of multiple isoforms. *J. Biol. Chem.* 279: 6401–6413.

Yu, C., Zhao, X., Qi, G., Bai, Z., Wang, Y., Wang, S., et al. (2017) Integrated analysis of transcriptome and metabolites reveals an essential role of metabolic flux in starch accumulation under nitrogen starvation in duckweed. *Biotechnol. Biofuels* 10: 167.

Zmijewski, J.W., Banerjee, S. and Abraham, E. (2009) S-glutathionylation of the Rpn2 regulatory subunit inhibits 26 S proteasomal function. *J. Biol. Chem.* 284: 22213–22221.